Journal of Physics: Conference Series **661** (2015) 012055 doi:10.1088/1742-6596/661/1/012055

Numerical simulation of heat fluxes in a two-temperature plasma at shock tube walls

E A Kuznetsov[1,2], **S A Poniaev**[2,3]

[1] Saint-Petersburg Polytechnical University
[2] Ioffe Physico-Techical Institute
[3] Mozhaikiy military space academy

Abstract. Numerical simulation of a two-temperature three-component Xenon plasma flow is presented. A solver based on the OpenFOAM CFD software package is developed. The heat flux at the shock tube end wall is calculated and compared with experimental data. It is shown that the heat flux due to electrons can be as high as 14% of the total heat flux.

1. Introduction

Supersonic flights give rise to high temperatures near surfaces of flying objects which are caused by a strong gas compression in front of a moving body and heat release due to internal friction in the gas. High temperatures give rise to nonequilibrium chemical properties of the gas flow, i.e., dissociation and recombination of gas molecules, atom ionization, and chemical reactions in the flow and at the flying object surface. Therefore, studies of supersonic gas flows should take into account these processes and variations in gas properties with temperature [1-5].

Particular attention in development of high-speed flying vehicles is paid to the choice of material and construction of the hull which is able to withstand high temperatures [1]. Thus, it is important to have a correct estimate of the heat flux at the flying object surface. To this end, modern mathematical models including the chemistry of gas flows and ionization and recombination of atoms and also modern numerical methods should be used.

The goal of our study was to simulate the inert gas plasma flows which are frequently used in experimental investigations of supersonic flows in shock tubes and to estimate heat fluxes at the shock tube wall and compare them with experimental data [2].

2. Mathematical model

We consider inert gas Xenon the plasma of which contains neutral atoms, electrons, and ions, i.e., we consider a three-component plasma. The electron gas temperature T_e differs from that of heavy particles (atoms and ions) T. The basic processes that determine the concentration of charged particles in the plasma are the electron impact ionization and three-body recombination [6]

$$Xe + e \rightleftharpoons Xe^+ + e + e. \quad (1)$$

Then the rate of electron concentration variation $\dot{n}_e$ is given by

$$\dot{n}_e = k_i n_e n_a - k_r n_e^3, \quad (2)$$

where k_i and k_r are the ionization and recombination coefficients, respectively, n_e is the electron concentration (which is equal to the ion concentration), and n_a is the atom concentration. The ionization and recombination coefficients are obtained by using a combined consideration of the ionization and recombination kinetics and population of excited states. The recombination coefficient k_r is the function of electron temperature. Fig. 1 shows the dependence of k_r on temperature for Xenon.

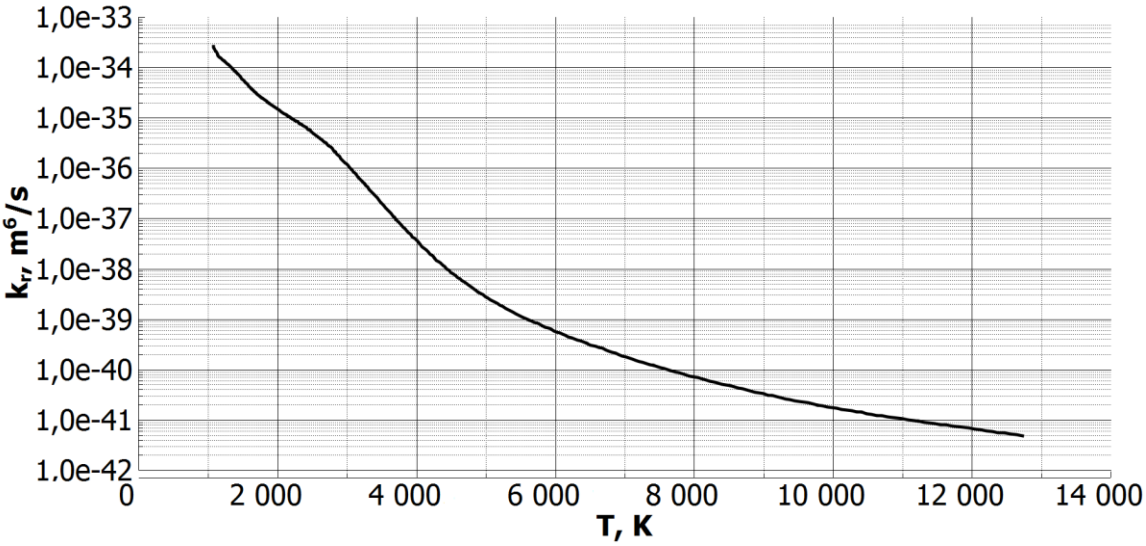

Figure 1. Recombination coefficient for Xenon as a function of temperature

The ionization coefficient k_i is found from the recombination coefficient by using the equilibrium constant K [6]

$$k_i = Kk_r \tag{3}$$

$$K = 1.936 \cdot 10^{22} \cdot T_e^{\frac{3}{2}} \cdot \exp\left(-\frac{140363}{T_e}\right) \tag{4}$$

There are many models which can be used to calculate the average collision frequencies between particles of different types [7]. In our simulation we used the models which seemed most appropriate for our case. We obtained the average frequencies of electron-ion and electron-atom collisions as

$$\nu_{ei} = n_e \frac{4\sqrt{2\pi}}{3}\left(\frac{m_e}{kT_e}\right)^{\frac{3}{2}}\left(\frac{e^2}{4\pi\varepsilon_0 m_e}\right)^2 ln\Lambda \cong 3.64 \cdot 10^{-6} n_e \frac{ln\Lambda}{T_e^{\frac{3}{2}}} \tag{5}$$

$$\Lambda = 1.24 \cdot 10^7 \left(\frac{T_e^{\,3}}{n_e}\right)^{\frac{1}{2}} \tag{6}$$

$$\nu_{ea} = n_a \frac{4}{3}\left(\frac{8kT_e}{\pi m_e}\right)^{\frac{1}{2}} \sigma_{ea} \tag{7}$$

where m_e is the electron mass, e is the electron charge and σ_{ea} is the collision cross-section given by

$$\sigma_{ea} = a_0^2(-1.82 + 2.2 \cdot 10^4 T_e^{-1} + 3.8 \cdot 10^{-7} T_e^2) \tag{8}$$

where $a_0 = 0.529 \cdot 10^{-10}$ m is the radius of first Bohr orbit.

Each component of the plasma mixture can be regarded as an individual medium that interacts with other components. Each one-component medium is described by a system of equations that express the laws of conservation for the continuum. It is necessary to include into this system of equations the terms that describe the interaction between one-component media. As a result, we have a system of equations for a two-temperature three-component plasma

$$\frac{\partial \rho}{\partial t} + \nabla \cdot \left(\rho \vec{V}\right) = 0 \tag{9}$$

$$\frac{\partial n_e}{\partial t} + \nabla \cdot \left(n_e \vec{V}\right) = \dot{n}_e \tag{10}$$

$$\frac{\partial (\rho \vec{V})}{\partial t} + \nabla \cdot \left(\rho \vec{V}\vec{V} + P\right) = 0 \tag{11}$$

$$\frac{\partial E}{\partial t} + \nabla \cdot \left(E\vec{V}\right) = -P\nabla \cdot \vec{V} - \nabla \cdot \vec{q} + \dot{n}_e \varepsilon_i + 3\frac{m_e}{m_a} k n_e (\nu_{ei} + \nu_{ea})(T_e - T) \tag{12}$$

$$\frac{\partial}{\partial t}\left(\frac{3}{2} p_e\right) + \nabla\left(\frac{5}{2} p_e \vec{V}\right) - \vec{V} \cdot \nabla p_e = -\nabla \cdot \overrightarrow{q_e} - \dot{n}_e \varepsilon_i - 3\frac{m_e}{m_a} k n_e (\nu_{ei} + \nu_{ea})(T_e - T) \tag{13}$$

$$\vec{q} = \lambda \nabla T \tag{14}$$

$$\overrightarrow{q_e} = \lambda_e \nabla T_e \tag{15}$$

$$\lambda_e = \frac{2.4}{1 + \frac{\nu_{ei}}{\sqrt{2}(\nu_{ei} + \nu_{ea})}} \cdot \frac{k^2 n_e T_e}{m_e (\nu_{ei} + \nu_{ea})} \tag{16}$$

where ρ is the flow density, $\vec{V}$ is the flow velocity vector, P is the pressure tensor, E is the flow energy, $\vec{q}$ is the heat flux due to heavy particles, ε_i is the ionization energy, m_a is the atom mass, p_e is the electron pressure, $\overrightarrow{q_e}$ is the heat flux due to electrons, λ is the heat conductivity of the material, and λ_e is the electron heat conductivity.

To solve the system of equations we obtained, we used the free, open source CFD software package OpenFOAM [8]. This allowed us to carry out operations with scalar, vector, and tensor fields in the framework of the finite-volume method.

One of important features of OpenFOAM is the possibility to make one's own utilities and solvers. OpenFOAM includes different solvers which are commonly accepted for the solution of one-temperature gas flows. So our solver for the solution of the two-temperature three-component plasma flow was built by adding additional equations and terms of equations to one of the available solvers for the one-temperature model.

3. Calculation results

In order to compare the results of numerical modulation and experimental data, we calculated the supersonic Xenon flow in the shock tube 10 cm in diameter with a section length of 0.5 m. The Mach number of the shock wave in the shock tube was 6. The calculations were performed for the two-dimensional axisymmetric case. The computational region is presented in Fig.2.

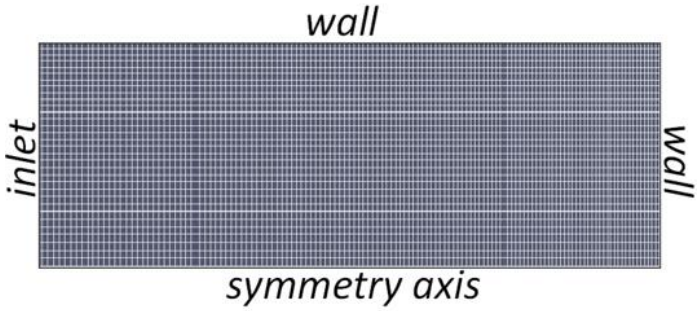

Figure 2. Computation region and mesh

The gas parameters in the low-pressure chamber of the shock tube were as follows: velocity - 0 m/s, gas pressure - 2235 Pa, temperature $T = T_e = 293$ K, and $n_e = 0$ m^{-3}. After the shock wave passed through the gas in the low-pressure chamber and gas ionization occurred, the gas parameters became as follows: velocity - 770 m/s, pressure - 10^5 Pa, $T = T_e = 3552$ K, $n_e = 2.17 \cdot 10^{17}$ m^{-3}.

Figures 3 and 4 show simulated and experimental heat fluxes [9,10] at the shock tube wall, respectively. It can be seen that the results of simulation and experimental data on the heat flux value at the shock tube end wall are in fairly good agreement when the heat flux reaches an approximately stationary level of 1400 kW/m^2. As one can see from Fig.3, there are two heat fluxes: q_T is the heat flux due to heavy plasma components and q_{Te} is the heat flux due to electrons (q is the total heat flux at the wall). The value of q_{Te} reaches approximately 14% of the total heat flux.

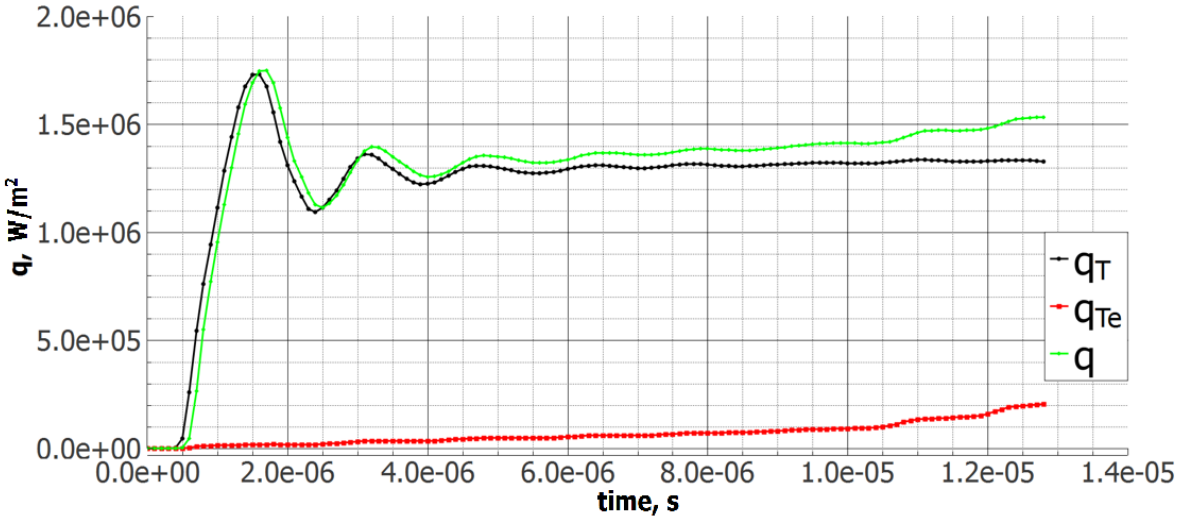

Figure 3. Simulation of heat flux at the shock tube end wall

No satisfactory agreement was found in the simulated and experimental temporal behaviors of the heat flux. This can be explained by the fact that some effects in the high-temperature gas were not taken into account in our simulation, and the processes at the shock tube turned out to be quicker in the simulation than in the experiment. For example, the length of the low-pressure chamber was 10 m and there a boundary layer developed near the walls in the experiment, while the simulation was performed for a 0.5-m long section which could be insufficient for a viscous flow development. It can also be important that in the simulation a change in gas parameters in the shock wave was an instantaneous process, and in reality it took some time to occur.

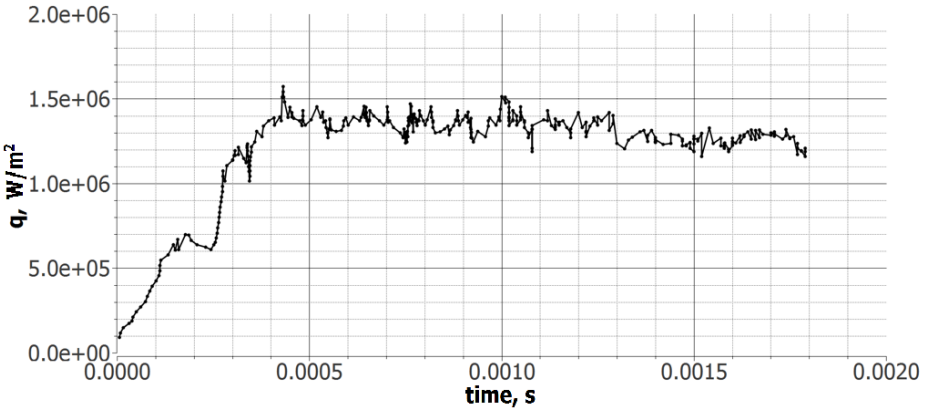

Figure 4. Experimental data on heat flux at the shock tube end wall

Conclusion

Numerical simulation has shown that the solver we have made can be used to estimate pulsed heat fluxes in the flows with different temperatures of heavy plasma particles and electrons. It can be used to calculate heat fluxes at the bodies flowed around by the supersonic flow created in the nozzle connected with the shock tube or arc-heated facilities. Model gases, such as Argon and Xenon, are frequently used in such investigations, and it is necessary to take into account the nonequilibrium ionization state and the two-temperature nature of the plasma flows. As shown above, the heat flux due to electrons can constitute a significant portion of the total heat flux.

References

[1] Edney B E *AIAA Journ.* 1968. V. **6**. N 1. P. 16-24.
[2] Sapochnikov S Z, Mitiakov V Y, Mityakov A V, Measurements of nonstationary heat fluxes by gradient sensors based on single-crystalline anisotropic bismuth, *Technical physics*, 2004, vol. 49, issue 7, pp 920-926
[3] Friedman H S and Fay J A Heat Transfer from Argon and Xenon to the End Wall of a Shock Tube *Physics of Fluids*, Vol. **8**, No. 11, 1965, pp. 1968-1975.
[4] Nowak R J and Yuen M C Heat Transfer to a Hemispherical Body in a Supersonic Argon Plasma *AIAA J.*, Vol. **11**, No. 11, 1973, pp. 1463–1464.
[5] Dillion R E and Nagamatsu H.T. Heat Transfer and Transition Mechanism on a Shock-Tube Wall *AIAA J.*, Vol. **22**, No. 11, 1982, pp. 1524-1528.
[6] Mitchner M and Kruger C, 1973, Partially ionized gases, Wiley, 518 p.
[7] Chernyi G G, Losev S A, Macharet S O, Potapkin B V, Physical and chemical processes in gas dynamics, 2002, Progress in Astronautics and Aeronautics, vol. 196
[8] OpenFOAM: the open source CFD toolbox. – http://www.openfoam.com
[9] Bobashev S V, Mende N P, Popov P A, Reznikov B I, Sakharov V A, Measurements of convective heat fluxes by sensors based on anisotropic thermal elements in pulsed gasdynamic processes, 2012, AIAA Paper 2012-0263
[10] Bobashev S V, Golovachov Y P, Mende N P, Reznikov B I, Popov P A, Sakharov V A, Schmidt A A, Chernyshev A S, Sapozhnikov S Z, Mityakov V Y, Mityakov AV, Application of the gradient heat flux sensor to study pulsed processes in a shock tube, 2008, Tech. Phys., v.53, 12, pp 1634-1635